

EXERCISE #2

OBSERVABILITY AND UV COVERAGE

Damien Ségransan¹

Abstract. This exercise is divided into two main parts. The first one intends to give a clear idea about the UV coverage with baselines of different orientations and targets of different declinations. It also emphasizes on the delay lines constraints for a 2 and a 3-telescope array. In the second part, different array configurations have to be selected to efficiently measure the radius of 3 close M dwarfs and the parameters (ρ , Θ , Δmag) of a binary system.

1 Sampling the UV plane with the VLT

First load the catalog named pws2a.sou. It contains 7 stars of R.A. 09:10:00 and of different declination. These prototype stars pass the meridian the 5th of February 2002 at midnight at Paranal. In this section an intensive use of the **OBSERVABILITY/COVERAGE** menu of **ASPRO** will be made. In the different widgets, select a **minimum elevation of 40 degrees and an hour angle range of -3h to +3h**.

1.1 UV tracks for a North-South baseline

Select a 2 telescope baseline oriented N-S (**WHERE** and **OBSERVABILITY/COVERAGE**).

Visualize the observability of the sources with/without delay lines constraints (**OBSERVABILITY/COVERAGE**). Plot the uv coverage for several stars and change the fixed delay. Why are the uv-tracks almost straight?

1.2 UV tracks for an East-West baseline

Select a large 2 telescope baseline oriented E-W. Visualize the observability of the targets with/without delay lines constraints. Plot the uv coverage for several stars

¹ Observatoire de Genève, 51 chemin des Maillettes, CH-1290, Sauverny, Switzerland

and change the fixed delay. Why are the uv-tracks elliptical? Have a look at the uv-tracks for a star with $\delta > 0$, $\delta = 0$ and $\delta < 0$. What do you notice?

Compare the N-S baseline and the E-W baseline in terms of UV-coverage, observability (how much UV-track is covered with the same fixed delay?)

1.3 UV tracks for a 3-telescope-array

Select a large 3 telescope array configuration. Visualize the observability of the targets with/without delay lines constraints. Plot the uv coverage for several stars and change the fixed delay. What can be noticed?

In which case is it important to observe with three telescopes?

2 Radius measurements and binary parameter determination

2.1 Direct radius measurement

Until very recently, only two M dwarf radii had been directly measured with great accuracy. This was done in the peculiar case of the eclipsing binary YYgem. Direct radius measurements of a few M dwarfs have been conducted very recently with success at PTI. The VLTI will be able to directly measure the radii of the closest M dwarfs thanks to its longest baseline ($> 100m$).

Table 1. Star main characteristics

Object	Spectral Type	Distance [pc]	J	Ra	Dec	Diameter [mas]
G1887	M0V	3.3	4.16	23:05:52	-35:51:11	1.69
G1551	M5.5V	1.3	5.28	14:29:42	-62:40:46	1.43
G1752B	M8V	5.9	9.9	19:16:57	+05:08:49	0.16

In this part load the catalog named pws2b.sou. Select an instrument and the photometric band. Also select an observing period, an optimal array configuration to determine their radius with the best accuracy. In this section an intensive use of the **WHAT & Object Model** menu and the **OBSERVABILITY/COVERAGE** menu of **ASPRO** will be made. In the different widgets, select a **minimum elevation of 40 degrees and an hour angle range of -3h to +3h**. Use the appropriate uniform disk model (see model section at the end of the document for model syntax and its analytical expression) to either display the amplitude, the phase of the visibility or the derivatives with respect to the diameter to visualize which part of the UV plane really constrain the model.

Is it possible to determine the radius of these stars?

Is it possible to determine phenomena that occur at higher frequencies like limb darkening?

Some of the late M dwarfs are fast rotators. Propose an observing strategy to efficiently detect a possible asymmetry of the star due to rotation.

2.2 Binary parameter determination

2.2.1 A binary star

First load/re-load the catalog named pws2a.sou and then select star number 4. This star goes through the meridian on the the 5th of February 2002 at midnight at Paranal. Let us consider it is a binary system with properties summarized in the following table.

Table 2.

Ra	Dec	ρ [mas]	P.A. [deg.]	Δ mag
9:10:00	+10:00:00	3	86	3

Select baseline G2 G1

Visualize the uv coverage and the amplitude. Does this baseline constrain the parameters of the binary?

Select baseline A0 M0

Visualize the amplitude, the phase, and their derivatives.

Does this baseline constrain the parameters of the binary?

What do you notice about the baseline orientation with respect to the binary system Position Angle?

2.2.2 The very low mass star G1866AC

G1 866ABC is a triple system with very low masses. The component G1866AC-B is resolved by adaptive optics and accurate radial velocities have been obtained for each component. From radial velocities, we can estimate the separation of the closest pair, G1866AC. However, the Position Angle is not known. The magnitude difference is expected to be close to zero.

Select an observing period and an optimal array configuration to determine the orbital parameters with the best accuracy. Use the appropriate **binary + uniform disk model** to display the amplitude or the phase of the visibility or the derivatives to visualize which part of the UV plane really constrain the model.

Is it possible to determine the parameters of the binary?

Is it possible to determine the radius of these stars?

Table 3. The values given for ρ , θ , Δmag and radii are expected values

Object	Spectral Type	Dist. [pc]	J	Ra	Dec	ρ [mas]	Δmag	radii
G1866AC	M7V	3.45	6.53	22:38:33	-15:18:06	7.4	0.0	0.27

3 Material

ASPRO and the catalogs named pws2a.sou and pws2b.sou are needed. It is assumed that loading catalogs and select an observing date and time are known.

3.1 Catalogs

Table 4. pws2a.sou

STAR1	9:10:00.000	70:00:00.000
STAR2	9:10:00.000	50:00:00.000
STAR3	9:10:00.000	30:00:00.000
STAR4	9:10:00.000	10:00:00.000
STAR5	9:10:00.000	-10:00:00.000
STAR6	9:10:00.000	-20:00:00.000
STAR7	9:10:00.000	-30:00:00.000
STAR8	9:10:00.000	-50:00:00.000
STAR9	9:10:00.000	-70:00:00.000

Table 5. pws2b.sou

G1551	23:05:52	-35:51:11
G1887	14:29:42	-62:40:46
G1752B	19:16:57	+05:08:49
G1866AC	22:38:33	-15:18:06

4 Appendix

4.1 Uniform Disk

The intensity distribution of a uniform disk is given in equation 4.1.

$$I(r) = I_s \Pi(r/D) \quad (4.1)$$

where D is the apparent diameter of the disk expressed in arcseconds. The Fourier transform of this radial function is:

$$\hat{I}(B/\lambda) = I_s 2 \frac{J_1(\pi B D / \lambda)}{\pi B D / \lambda} \quad V(|\mathbf{f}|) = 2 \frac{J_1(\pi |\mathbf{f}| D)}{\pi |\mathbf{f}| D}$$

where $\mathbf{f} = \mathbf{B}D/\lambda$. It should be noticed that the visibility of a uniform disk model is real and has π phase shifts at $\mathbf{f}D = 1.22, 2.33, 3.33, \dots$

4.2 Limb Darkened Disk

Limb darkening is usually represented as follows:

$$\frac{I(\mu)}{I(1)} = 1 - \sum_{i=1}^N \alpha_i (1 - \mu)^{\beta_i} \quad (4.2)$$

where μ is cosine of the angle between the photosphere and the vector pointing into the source direction, $I(1)$ is the intensity at the center of the star, α_i are the limb darkening coefficients and $\beta_i = i$ or $i/2$, depending on models. The value of N also depends on models.

The visibility of a limb darkened disk is:

$$V(|\mathbf{f}|) = \frac{\int_0^1 I(\mu) J_0(|\mathbf{f}| \pi D (1 - \mu^2)^{1/2}) \mu d\mu}{\int_0^1 I(\mu) \mu d\mu} \quad (4.3)$$

4.3 Binary star

The intensity distribution of a binary star is:

$$I(\mathbf{x}) = I_1 \delta(\mathbf{x}) * \Pi(r/D_1) + I_2 \delta(\mathbf{x} - \mathbf{x}_2) * \Pi(r/D_2) \quad (4.4)$$

Its Fourier transform is:

$$\hat{I}(B/\lambda) = I_1 2 \frac{J_1(\pi B D_1 / \lambda)}{\pi B D_1 / \lambda} + I_2 2 \frac{J_1(\pi B D_1 / \lambda)}{\pi B D_1 / \lambda} \exp(-2i\pi \mathbf{B} \Delta \mathbf{X} / \lambda) \quad (4.5)$$

If one defines q as the flux ratio between the secondary and the primary star, $q = \frac{I_2}{I_1}$, and \bar{V}_i as the individual star visibility i then $\bar{V}_i = \frac{J_1(\pi |\mathbf{f}| D_i)}{\pi |\mathbf{f}| D_i}$, and the

resulting visibility is the following, while the squared visibility is given by equation 4.7:

$$V(\mathbf{f}) = \frac{1}{1+q} (\bar{V}_1 + q \bar{V}_2 \exp(-2i\pi\mathbf{f}\Delta\mathbf{X})) \quad (4.6)$$

$$|V(\mathbf{f})|^2 = \frac{1}{(1+q)^2} (\bar{V}_1^2 + q^2 \bar{V}_2^2 + 2q\bar{V}_1\bar{V}_2 \cos(2\pi\mathbf{f}\Delta\mathbf{X})) \quad (4.7)$$

4.4 Simple models with ASPRO

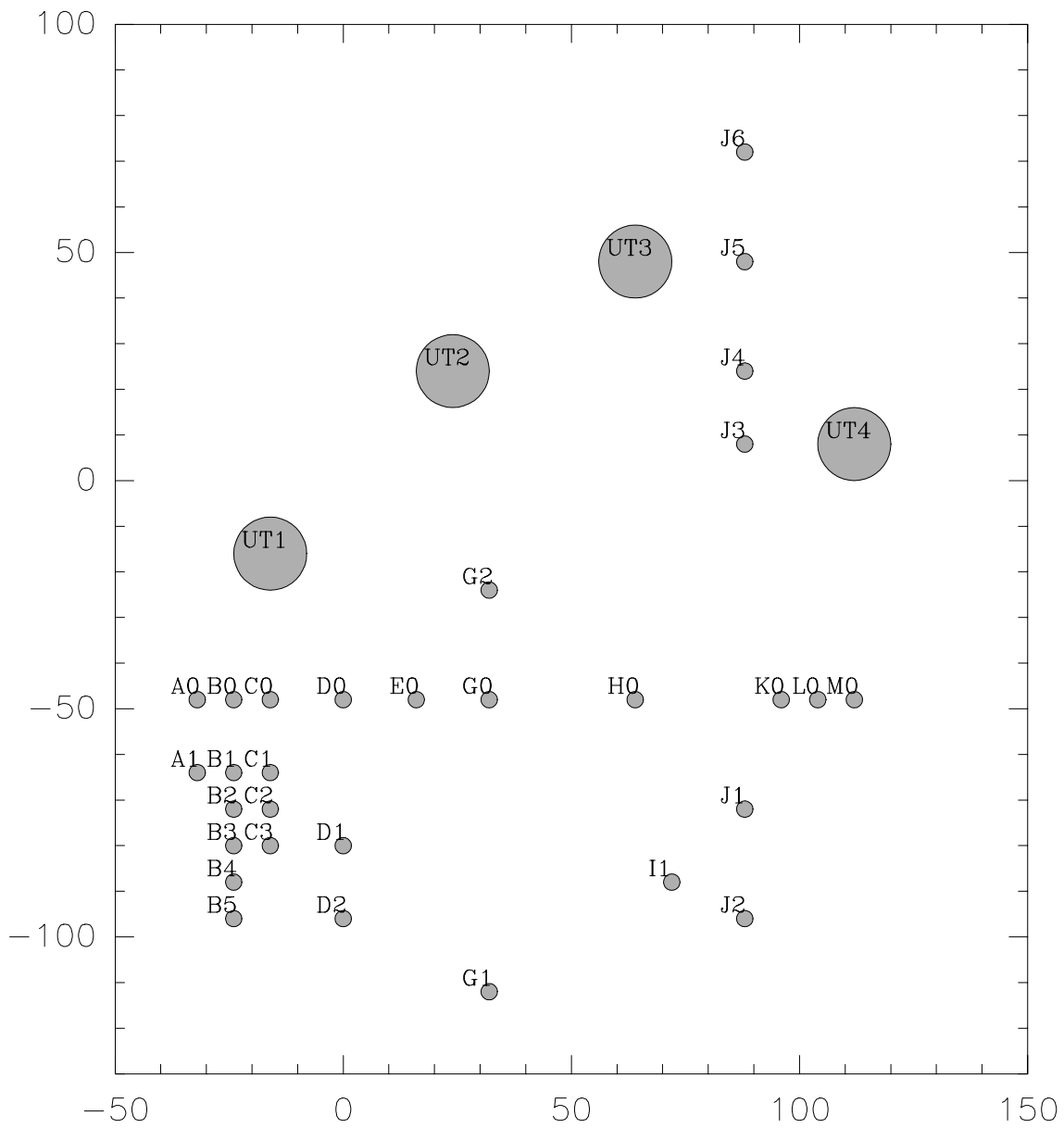
The task **Object Model** in ASPRO, allows to write models directly into a visibility table. The models are either simple or linear combinations of several functions. Currently supported distributions and parameters (aside offset in arc second from the maps center and flux) are:

POINT	Point source	None
E_GAUSS	Elliptic Gaussian source	FWHP Axis (Major and Minor), Pos Ang
C_GAUSS	Circular Gaussian source	FWHP Axis
C_DISK	Circular Disk	Diameter
E_DISK	Elliptical (inclined) Disk	Axis (Major and Minor), Pos Ang
RING	Ring	Inner Ring Diameter, Outer ring diam
U_RING	Unresolved Ring	Diameter (1 value: unresolved!)
EXPO	Exponential brightness	FWHP Axis
POWER-2	$B = 1/r^2$	FWHP Axis
POWER-3	$B = 1/r^3$	FWHP Axis
LD_DISK	Limb-Darkened Disk	Diameter, 'cu' and 'cv'
BINARY	Binary	Flux ratio, rho, theta

POINT	Offset R.A.	Offset Dec	Flux	-	-	-
E_GAUSS	Offset R.A.	Offset Dec	Flux	Maj. diam.	Min. diam.	Pos Ang
C_GAUSS	Offset R.A.	Offset Dec	Flux	Diameter	-	-
C_DISK	Offset R.A.	Offset Dec	Flux	Diameter	-	-
E_DISK	Offset R.A.	Offset Dec	Flux	Maj. diam.	Min. diam.	Pos Ang
RING	Offset R.A.	Offset Dec	Flux	Inner Diameter	Outer Diameter	-
U_RING	Offset R.A.	Offset Dec	Flux	Diameter	-	-
EXPO	Offset R.A.	Offset Dec	Flux	Diameter	-	-
POWER-2	Offset R.A.	Offset Dec	Flux	Diameter	-	-
POWER-3	Offset R.A.	Offset Dec	Flux	Diameter	-	-
LD_DISK	Offset R.A.	Offset Dec	Flux	Diameter	'cu' and 'cv'	-
BINARY	Offset R.A.	Offset Dec	Flux	FluxRatio	Rho	Theta

Table 6. Note: for the Binary model, the flux ratio is Flux_secondary/Flux_primary and Rho & Theta are the angular separation (") and Position angle (degrees) of the binary.. **Offset R.A.** and **Offset Dec** are usually set to zero while **flux** is set to one.

4.5 Baselines

**Fig. 1.** VLTi stations

Length (m)	Name(s)
8	B0-A0,B0-C0,B1-A1,B1-C1,B2-C2,B3-C3,K0-L0,M0-L0,B2-C1,B3-C2,B4-C3,B1-C2,B2-A1,B2-C3
16	A0-C0,A1-C1,D0-C0,D0-E0,D1-C3,E0-G0,K0-M0,B0-A1,B1-C0,B3-C1,B4-C2,B5-C3,B0-C1,B1-A0,B1-C3,B3-A1,A1-C2,D1-C2,I1-J2
24	A1-C0,D0-C1,I1-J1,A0-C1,A1-C3,D1-C1,D2-C3,B0-D0,D1-B3,D2-B5,J3-UT4,UT3-J5,G2-G0,B2-D1,D2-B4,D1-B4,B2-C0,B4-C1,B5-C2,K0-J1,B0-C2,B2-A0,B4-A1
32	B1-D0,D1-B5,D0-C2,G2-E0,J1-L0,A0-C2,D2-C2,B1-D1,B3-D2,UT4-J4,C0-E0,D0-A0,D0-G0,G0-H0,K0-H0,UT1-C0,B0-UT1,B3-C0,B5-C1,B0-C3,B3-A0,B5-A1,D0-B2,J6-UT3,M0-J1,B2-D2,H0-J1,UT3-J4
40	C1-E0,D0-A1,A0-UT1,D0-C3,D1-E0,A0-C3,D0-UT1,D1-C0,D2-C1,D1-A1,G1-D2,B0-E0,H0-L0,E0-C2,G2-D0,D0-B3,B0-D1,B1-D2,G2-H0,B4-C0,B4-A0,I1-H0,B1-E0
48	D1-G0,E0-C3,D1-A0,D2-A1,G1-D1,UT1-E0,B2-E0,G1-I1,UT2-UT3,D0-B4,I1-K0,UT3-J3,UT4-J5,A0-E0,C0-G0,E0-H0,M0-H0,UT1-C1,G2-UT1,B1-UT1,B5-C0,K0-J2,B5-A0,G2-UT2,A1-E0,C1-G0,D2-E0,L0-J2,UT1-A1,D2-C0,B3-E0,I1-L0
56	C2-G0,G2-C0,D0-B5,M0-J2,B0-D2,H0-J2,B0-G0,M0-UT4,UT1-C2,B4-E0,I1-M0,UT1-UT2,B2-UT1,L0-UT4,K0-J3,G0-I1,C3-G0,D2-G0,D2-A0,G1-C3,UT1-G0,G1-B5,B1-G0,G1-J2,K0-UT4,L0-J3
64	B2-G0,G2-B0,H0-J3,M0-J3,G0-J1,G1-B4,G2-C1,B5-E0,G1-C2,UT3-UT4,A0-G0,D0-H0,G0-K0,UT2-J4,UT1-C3,B3-G0,G2-J3,G2-D1,B3-UT1,G1-B3,UT2-J3,A1-G0,D1-UT1,G1-E0
72	G2-C2,G1-C1,G2-A0,UT2-J5,J6-UT4,G2-K0,B4-G0,G1-J1,G2-B1,E0-I1,G1-B2,D1-H0,G1-H0,G1-D0,G0-L0,D1-I1,D2-I1,B4-UT1,UT2-E0,K0-J4,UT2-G0,B5-G0,G2-B2,G2-J4,G2-C3,H0-UT4,L0-J4,G0-J2,G1-B1,G2-J1,G2-A1,G2-I1
80	E0-J1,G2-L0,D0-UT2,H0-J4,M0-J4,G2-D2,G2-UT3,G0-J3,G2-B3,C0-H0,E0-K0,G0-M0,D2-H0,UT2-J6,J1-J3,G1-C0,G1-A1,B5-UT1,C1-H0,D2-UT1,C0-UT2,UT2-H0,D0-I1
88	G2-M0,C2-H0,J1-UT4,G2-B4,G1-B0,C3-H0,G2-UT4,UT1-H0,B0-UT2,E0-J2,B0-H0,D2-J2,E0-L0,G1-G2,C3-I1,D1-J1,C2-I1,D1-J2,UT2-UT4,B1-H0,G1-K0,G1-A0,C1-I1,D0-J1,B2-H0,D2-J1,E0-J3,A0-UT2,G0-J4,G2-J5,G2-B5,G2-J2
96	B3-H0,A0-H0,B4-I1,D0-K0,E0-M0,H0-UT3,J1-J4,B3-I1,B5-I1,G1-L0,K0-J5,B4-H0,UT2-C1,C0-I1,B2-I1,A1-H0,I1-J3,L0-J5,G0-UT4,B1-I1,H0-J5,M0-J5
104	B5-H0,B1-UT2,D0-J2,D1-K0,G0-UT3,K0-UT3,E0-J4,UT2-K0,G1-M0,UT1-UT3,C2-J1,D0-L0,I1-UT4,UT2-C2,J2-J3,L0-UT3,B0-I1,C1-J1,C3-J1,D0-J3,A1-UT2,C3-J2,A1-I1,C0-J1,C2-J2,UT1-J3,D1-UT2,J2-UT4,D2-K0,B2-UT2,E0-UT3,G1-UT1,M0-UT3
112	UT2-L0,C1-J2,D1-L0,E0-UT4,G0-J5,G2-J6,UT1-J4,UT2-C3,A0-I1,B2-J1,B5-J2,C0-K0,D0-M0,B1-J1,B4-J2,B3-J1,B3-J2,B4-J1,C1-K0,I1-J4,D0-J4,UT1-I1,UT2-M0,B0-J1,B2-J2,B5-J1,C2-K0,D2-L0,B3-UT2,C0-J2,D0-UT3,UT2-J1
120	B1-J2,UT1-K0,C3-K0,D1-M0,C0-J3,UT1-J1,B0-K0,C0-L0,E0-J5,J1-J5,J2-J4,A1-J1,J6-K0,B1-K0,C1-L0,J6-L0,D2-M0,B4-UT2,UT2-I1,B0-J2,UT1-J5,A0-J1,B2-K0,C2-L0,D2-UT2,J6-H0,J1-UT3,J6-M0
128	A1-J2,UT1-L0,B3-K0,C3-L0,D1-J3,C0-UT3,B0-J3,D0-UT4,B4-K0,C0-J4,C1-J3,A0-K0,B0-L0,C0-M0,A1-K0,B1-L0,C1-M0,B5-K0,B5-UT2,A0-J2,B2-L0,C2-M0,UT1-UT4,B0-UT3,D0-J5,C2-J3,UT1-J2
136	UT1-M0,B3-L0,C3-M0,A0-J3,G0-J6,G1-J3,B0-J4,B1-J3,B4-L0,A0-UT3,A0-L0,B0-M0,UT2-J2,C1-J4,C3-J3,UT1-J6,D1-J4,D2-J3,G1-UT2,I1-UT3,B5-L0,A1-L0,B1-M0,I1-J5,B2-J3,C1-UT3,B2-M0
144	B3-M0,C0-UT4,A0-J4,A1-J3,E0-J6,C0-J5,C2-J4,B4-M0,B1-J4,B3-J3,D1-UT4,B1-UT3,D1-UT3,A0-M0,J2-J5,J6-J1,B5-M0,C2-UT3,G1-UT4,A1-M0,J2-UT3,C1-UT4,B0-UT4,C3-J4,G1-J4
152	B0-J5,B2-J4,B4-J3,A1-UT3,A1-J4,B2-UT3,D0-J6,D2-J4,C2-UT4,C3-UT3,B3-J4,B5-J3,D2-UT4,C1-J5,A0-J5,B1-UT4,A0-UT4,C3-UT4,B3-UT3,D1-J5
160	D2-UT3,B2-UT4,B1-J5,B4-J4,C0-J6,C2-J5,J6-I1,A1-UT4,B3-UT4,B4-UT3,G1-UT3
168	A1-J5,B0-J6,B2-J5,B5-J4,C3-J5,B4-UT4,J6-J2,B5-UT3,D2-J5,G1-J5,A0-J6,B3-J5,B5-UT4,C1-J6
176	D1-J6,B1-J6,B4-J5,C2-J6
184	A1-J6,B2-J6,B5-J5,C3-J6
192	B3-J6,D2-J6,G1-J6,B4-J6
200	B5-J6

Table 7. VLTI baselines sorted by length